restoration process exceeds a certain value, the system will go to that steady state. Such a steady state may be only marginally stable, so that the system can still be excited by a suitable perturbation.

In many of the known solution oscillators, this final process is escape of a gas. Many metabolic processes in living organisms produce carbon dioxide, which then affects cytoplasmic pH. If pH is important to the processes leading to oscillation, diffusive escape of carbon dioxide through cell walls could be the slow process permitting the delayed feedback necessary for oscillation.

We wish to emphasize the biological suggestions we have made above are purely speculative without any experimental justification. However, they arise from direct analogies with now established mechanisms in simpler chemical systems. We make no claim they are valid, but we believe they are provocative. We hope they will suggest further tests by which these crude ideas may be substantiated or rejected.

Notes Added in Proof

Bowers and Rawji[67] have also studied the Morgan reaction[42,43] of formic acid dehydration. They believe the oscillations are caused by physical rather than by chemical effects.

Bose, Ross, and Wrighton[68] have independently observed photochemically induced oscillations in the fluorescence of anthracene and of dimethylanthracene similar to those found by Turro[49] for the diphenyl derivative.

Much of the work described here was supported either by the National Science Foundation or by the Atomic Energy Commission.

(67) P. G. Bowers and G. Rawji, *J. Phys. Chem.*, submitted for publication.
(68) R. L. Bose, J. Ross, and M. S. Wrighton, *J. Am. Chem. Soc.*, submitted for publication.

A Transition-State Probe

Dudley H. Williams

University Chemical Laboratory, Cambridge, United Kingdom

Received February 2, 1977

A central problem in chemistry is that of increasing our knowledge of transition states. The lifetime of the transition state is so short relative to the time scale of the majority of our investigative techniques that direct observations are normally not possible. Thus, in solution chemistry, conclusions regarding transition-state geometry may be inferred from calculation following kinetic studies; the possibility of the *direct* measurement of a transition-state property is lost due to collisions which precede the determination of the experimental parameter (e.g., rate of product formation). Clearly, if we wish to obtain information about transition-state geometry, then it would be extremely useful to know what happens to the electronic energy stored in the stretched bonds of the transition state (e.g., 1) as it passes to more stable products (e.g., 2).

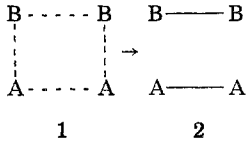

1 2

Let us consider first a hypothetical and extreme case where the geometry of 1 was such that the A–A and B–B bond lengths were close to their equilibrium values in the products 2, and the excess electronic energy of 1 over 2 could then be regarded as lying in the form of a potentially repulsive interaction along the two A--B bonds in 1. Thus, as the transition state was converted to products, a quantity of energy close to the reverse activation energy would appear as kinetic energy (mutual repulsion) of the products. In the reverse process (2 → 1), such a model would correspond to an activation energy being supplied by collision of A–A and B–B due to relative translation along the A → B directions, without the requirement of vibrational excitation of A–A and B–B.

As a second and opposite extreme, we might envisage a situation where the A–A and B–B bond lengths in 1 were far from their equilibrium values in the products 2, such that the excess electronic energy of 1 over 2 would appear as vibrational energy of the products 2, which would drift apart without mutual repulsion. Here, in the reverse process (2 → 1), the activation energy would be supplied almost exclusively as vibrational energy of A–A and B–B, a large relative translational (collisional) energy of the two molecules not being required.

Information on the presence or absence of large mutual repulsions of A–A and B–B as a transition state 1 collapses to products in a period comparable to vibrational frequencies (10^{-13} s) can only be obtained by direct observation of the behavior of isolated 1, i.e., in the absence of collisions. Such conditions can be found in a molecular beam. The measurement of mutual repulsion of two particles formed by the collapse of a transition state is facilitated if the transition state itself carries a charge and the products correspond to a charged molecule and a neutral molecule. The ionic product can then be passed through a magnetic field

Dudley H. Williams was born in Leeds, England, in 1937, and studied for his undergraduate and doctoral degrees at the University of Leeds. He subsequently worked at Stanford University as a postdoctoral fellow, and then returned to the U.K. to carry out research and teaching at Cambridge University. He is a Fellow of Churchill College and Reader in Organic Chemistry at the University of Cambridge. His research interests cover the general areas of structure elucidation and synthesis in organic chemistry, with special interest in the development and application of new techniques in mass spectrometry and nuclear magnetic resonance. He is a past recipient of the Meldola Medal of the Royal Institute of Chemistry and the Corday–Morgan Medal of the Chemical Society.

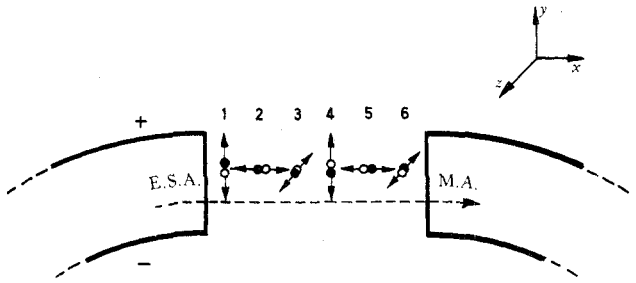

Figure 1. Schematic diagram showing the dissociation of an ion, m_1^+ (◐), to a product, m_2^+ (○), and a neutral (●). In the ideal case, kinetic energy release in the direction of the beam (x direction), in orientations 2 and 5, gives rise respectively to the high-mass and low-mass components shown in **3** in the text. The illustrations refer to reactions occurring in a double-focusing mass spectrometer, after the electric sector (E.S.A.) and prior to the magnetic analyser (M.A.).

in which its path will depend upon the momentum of the ion. It can be shown[1] that, for a dissociation occurring before the magnetic sector of a mass spectrometer, ions repelled in the direction of motion of the beam may readily be resolved from ions pushed back against the direction of the beam (Figure 1) if the repulsive energy (kinetic energy) released as the transition state collapses is a few kilocalories per mole or greater.

Mutual repulsion of products in the dissociation schematically depicted in Figure 1 actually leads to an exploding sphere of particles, but those exploding in a direction perpendicular to the direction of the beam are normally detected less efficiently at the detection device (collector). Some typical distributions of detected product ions are shown in **3** to **5**; we shall illustrate our

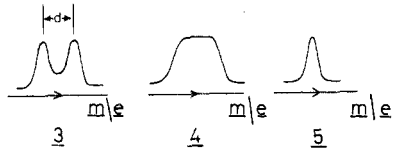

arguments in terms of a beam of molecules travelling from left to right. In the case of **3**, ions pushed along the direction of the beam occur at a higher position on the mass scale (m/e) than those pushed back against the direction of the beam; good resolution of these two kinds of ions is favored by (i) a relatively large kinetic energy release and (ii) an instrument with a high energy and angular resolution. The approximate energy release can be calculated[1] from the directly measured distance d (see **3**). If the energy release is smaller, or the energy resolution of the instrument lower, then a flat-topped peak may be observed (**4**). If a negligible, or very small, energy release occurs, or, more precisely, a small range of energies is released, then a relatively narrow gaussian peak (**5**) is observed.

Profiles of the type just described can in fact be observed in conventional mass spectra recorded on magnetic sector instruments. They are conventionally known as "metastable peaks". However, this term is neither a logical term nor descriptive of the physical effects which determine the peak shape; for the purposes of this account the profiles will be called energy-release profiles, although it is actually the square of the abscissa that gives the kinetic energy release.

The energy release profile of a chemical reaction will of course be most useful if, to a good approximation,

(1) J. H. Beynon and A. E. Fontaine, *Z. Naturforsch. A*, **22**, 334 (1967).

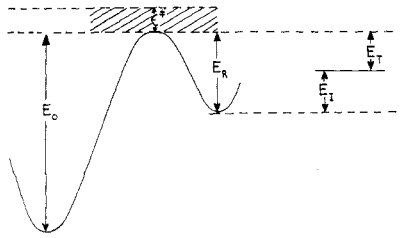

Figure 2. Potential surface for a one-step dissociation showing activation energy (E_0), excess energy in the transition state (ϵ^*), reverse activation energy (E_R), and partition of E_R into kinetic energy (E_T) and internal energy (E_I).

Table I
Some Primary Deuterium Isotope Effects Observed for Slow ("Metastable") Dissociations Occurring in the Mass Spectrometer

Precursor ion	Competing losses	Isotope effect[a]
$CHD_3^{+\cdot}$	$H\cdot/D\cdot$	$H\cdot$ loss only[4]
$CH_3CD_3^{+\cdot}$	$H\cdot/D\cdot$	600:1[5]
$C_2H_2D_3^+$	H_2/D_2	7.9:1.0[6]
$C_6H_2D_5^+$	H_2/D_2	3.0:1.0[6]

[a] Where necessary, a statistical correction for the differing numbers of H and D atoms present in the precursor ion has been made.

we are measuring only that fraction of the reverse activation energy which is converted to kinetic energy and not in addition some portion of a large excess energy (ϵ^*) which might happen to fluctuate into the reaction coordinate(s) as dissociation occurs (Figure 2). In other words, our experiment should be designed to sample only dissociating ions with energies slightly in excess of the minimum required for reaction (hatched region in Figure 2) and should not be concerned with ions containing large excess energies ϵ^*.[2] The conventional mass spectrometer is in fact well-suited to such restrictions since the ions which give rise to the energy-release profiles must survive some 10^8 vibrations after formation in order to be sampled during dissociation in front of the magnetic sector. Hence, since there are no collisions, the activation energy for reaction (E_0) is available from the time of ion formation, but the internal energy available is so little in excess of E_0 that 10^8 vibrations are necessary before it fluctuates into the appropriate bonds to bring about dissociation.

Dissociations some 10^8 vibrations after ion formation correspond to ion lifetimes of ca. 10 μs and rate constants (k) in the range 10^4–10^6 s^{-1}. (Note that such rate constants cannot usefully be directly compared with solution rate constants, which represent the reciprocal of mean lifetimes averaged over the Maxwell–Boltzmann distribution. Thus, the solution rate constants weight both species which do and do not react, whereas the rate constants quoted in the main text represent only the reciprocal of the mean lifetime of species which react.) Such reactions can, in favorable cases, be surprisingly "gentle" relative to the experience of the solution chemist. "Gentle" of course here refers to the relatively small depth of the hatched energy band in Figure 2 and not to E_0 itself, which is determined by the chemical nature of the dissociating species. For example, in the dissociations of $CHDCHD^{+\cdot}$ some 10^8 vibrations after ionization (hereafter called "slow" dissociations), the ratio of H_2:D_2 losses is approximately

(2) R. G. Cooks, J. H. Beynon, R. A. Caprioli, and G. R. Lester, "Metastable Ions", Elsevier, Amsterdam, 1973.

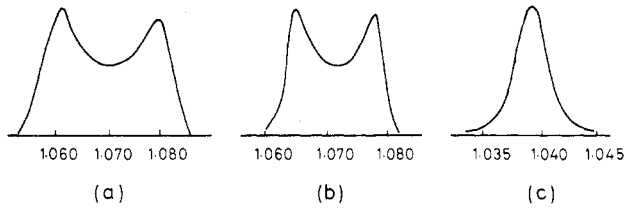

Figure 3. Energy-release profiles for loss of H_2 from (a) $CH_2{=}OH^+$, (b) $CH_2{=}NH_2^+$, and (c) $C_6H_7^+$. The peaks were recorded using the refocussing technique described by M. Barber and R. M. Elliott (12th Annual Conference on Mass Spectrometry and Allied Topics, Committee E.14, ASTM, Montreal, June 1964). The horizontal coordinates in the figure are V/V_0.

Table II
Energetics (kcal mol^{-1}) for the Reactions Given in Equations 1 and 2

Reaction	E_0	E_R	E_I	E_T
Eq 1	97	22	~2	20
Eq 2	80	52	19	33

700:1.[3] Some other isotope effects involving the stretching of C–H vs. C–D bonds in the transition state are given in Table I.

For those reactions so far quoted which show the largest isotope effects, the excess energies present in the transition states will be in the region of only 1 to 2 kcal mol^{-1}. Isotope effects of this magnitude are not found in solution kinetics since the whole Maxwell–Boltzmann distribution must be sampled, weighting not only "gentle" reactions (large isotope effect) but also those involving more excess energy (larger $\epsilon^{\ddagger}$ and smaller isotope effect). Frequently, the deuterium isotope effects for slow dissociations in our experiments[6] are comparable to those observed in solution reactions, indicating a slower rise of the rate constant with energy than for the larger isotope effects quoted above.

The One-Step Reaction

The surface shown in Figure 2 indicates that, if for a one-step reaction we know the heats of formation of both reactants and products and the forward activation energy (E_0), then we know the reverse activation energy (E_R) and our experiment will also give the partitioning of E_R between internal energy of products (E_I) and kinetic-energy release (E_T). In our work we have concentrated on the unimolecular reactions of closed-shell (even-electron) species of the type frequently involved as intermediates in organic reactions in solution, e.g., carbocations, protonated aldehydes and ketones, and protonated imines. Let us consider first the reactions shown in eq 1 and 2. Here there is no

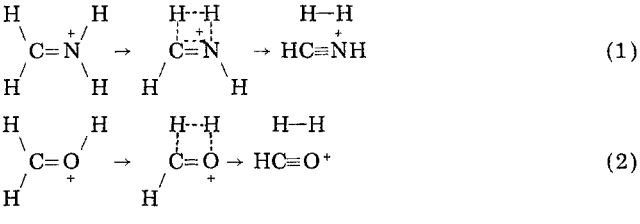

(1)

(2)

(3) I. Baumel, R. Hagemann, and R. Botter, 19th Annual Conference on Mass Spectrometry and Allied Topics, Committee E.14, ASTM, Atlanta, Ga., May 1971.
(4) L. D. Hills, M. L. Vestal, and J. H. Futrell, *J. Chem. Phys.*, **54**, 3834 (1971).
(5) V. Lohle and Ch. Ottinger, *J. Chem. Phys.*, **51**, 3097 (1969).
(6) G. Hvistendahl and D. H. Williams, *J. Chem. Soc., Chem. Commun.*, 4 (1975).

Scheme I

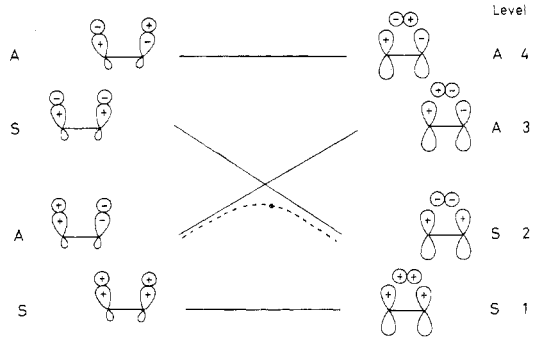

reasonable doubt as to the structure of either reactants or products nor as to the general nature of the transition states shown in the equations. For example, CD_3OH after ionization (by electron impact) loses a deuterium radical to produce $CD_2{=}OH^+$, which in slow dissociations specifically loses HD with an energy release profile (Figure 3a) corresponding to an energy release of 33 kcal mol^{-1}.[7,8] Similar restrictions apply to eq 1 (see also Figure 3b), and relevant data are given in Table II.[8]

It is striking that the barriers to these 1,2 eliminations of H_2 are very high (97 and 80 kcal mol^{-1}, respectively) and that a large fraction of the reverse activation energy is released as kinetic energy. From our earlier considerations, we have seen that a generalized expectation is that a reaction will occur with kinetic-energy release if an activated complex is at, or passes toward, product-like molecules which are at sufficiently close distances to experience mutual repulsion. Such a situation could arise in different ways, and in this respect it is noteworthy that the reaction given in eq 1 is isoelectronic with the four-electron symmetry forbidden reaction[9] $H_2C{=}CH_2 \rightarrow HC{\equiv}CH + H_2$. The correlation diagram which is relevant to such a reaction is given in Scheme I.[8]

In such reactions, four electrons of two σ (X–H) bonds (X = C, N, O) [left-hand side (LHS) of Scheme I] become two σ electrons of H_2 and two π electrons of the other product [right-hand side (RHS) of Scheme I]. In the reactant, these four electrons occupy the two molecular orbitals associated with levels 1 and 2; those associated with levels 3 and 4 are unoccupied. In comparing molecular orbitals of reactants and products, orbitals of like symmetry are connected by solid lines. It can be seen that, if the electrons in the reactant orbitals simply passed into product orbitals of like symmetry, then level 3 of the products would be occupied at the expense of level 2, i.e., the products would be produced in an electronically excited state. However, taking for example eq 2, it is clear that the products are not produced in an electronically excited state since, after allowing for the kinetic-energy release (33 kcal mol^{-1}), the internal energy of products is only ~19 kcal mol^{-1} above the sum of heats of formation of the ground-state products. Hence in the real reaction, as it proceeds, the electronic energy of the system initially rises rapidly due to the $2A_{LHS} \rightarrow 3A_{RHS}$ correlation, but

(7) J. H. Beynon, A. E. Fontaine, and G. R. Lester, *Int. J. Mass Spectrom. Ion Phys.*, 1, 1 (1968).
(8) D. H. Williams and G. Hvistendahl, *J. Am. Chem. Soc.*, **96**, 6753 (1974).
(9) R. B. Woodward and R. Hoffmann, *Angew. Chem., Int. Ed. Engl.*, 8, 797 (1969).

as the transition state is reached two electrons pass into the orbital described by the $3S_{LHS} \rightarrow 2S_{RHS}$ correlation. Examining the properties of the system at this point along the reaction coordinate (see • in Scheme I), we see that the electronic energy of the system is high because the $2S_{RHS}$ molecular orbital is characterized by a strong mutual repulsion of H_2 and the product ion at relatively small r (see **6**). Such symmetry-forbidden

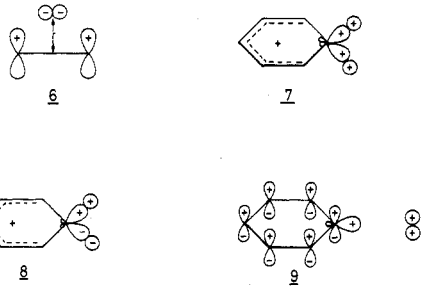

reactions should therefore occur with a large kinetic-energy release, as is observed experimentally.

When one-step reactions can proceed smoothly to products through symmetry-allowed routes where $\sum\Delta H_f$ for the products is greater than ΔH_f of the reactant, then it may often be the case that the reaction will not involve a large reverse activation energy, and then of course a large kinetic-energy release is precluded. This situation appears to hold for the only slow unimolecular dissociation of protonated benzene, which produces $C_6H_5^+$ and H_2.[10,11] This reaction is again a four-electron process in which four electrons of two σ(C–H) bonds become two σ electrons of H_2 and two π electrons (out of six π electrons) of the phenyl cation. The relevant symmetric (with respect to the plane of the ring) orbital of $C_6H_7^+$ is shown in **7**, and the slightly higher energy antisymmetric orbital is shown in **8**; the two electrons of the symmetric orbital shown in **7** can pass into the symmetric orbital of H_2 (see **9**), whereas those of the antisymmetric orbital shown in **8** can pass into the antisymmetric π system to produce the aromatic ring of **9** (by addition to the four π electrons of the dienyl cation). The reaction is symmetry allowed, and the reaction profile for this dissociation (Figure 3c)[10] does indeed show no large and specific kinetic-energy release. This situation is pleasing since, if a film of the reaction were run backwards, we should see the reverse reaction proceeding initially as the "solvation" of the empty orbital of the phenyl cation by H_2—a process which quite plausibly should not require a large translational energy of H_2.

On the basis of the above analysis, it appears that the most facile unimolecular reaction of the ethyl cation (H_2 loss) is a symmetry-allowed 1,1 elimination, since the reaction gives rise to a very narrow energy-release profile.[11] Again, a 1,1 elimination from an sp^3 carbon adjacent to a vacant p orbital leads to a vinylium ion as product.

(10) D. H. Williams and G. Hvistendahl, *J. Am. Chem. Soc.*, **96**, 6755 (1974).

(11) G. Hvistendahl and D. H. Williams, *J. Chem. Soc., Perkin Trans. 2*, 881 (1975).

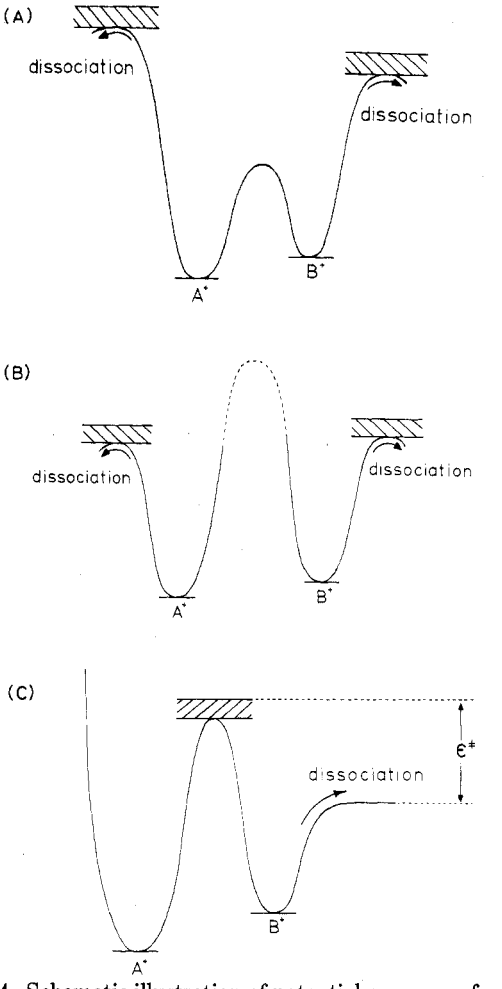

Figure 4. Schematic illustration of potential-energy surfaces for unimolecular reactions of A^+ and B^+. At the energies appropriate to dissociation after 10^8 vibrations (a) A^+ and B^+ rapidly interconvert, (b) A^+ and B^+ behave independently, and (c) A^+ undergoes slow isomerization to B^+.

A similar analysis leads to the prediction[10] that $CH_5^+ \rightarrow CH_3^+ + H_2$ will occur without a large and specific kinetic-energy release, as has subsequently been established.[12]

Multi-Step and Potentially Multi-Step Reactions

In considering two-step or potentially two-step reactions, it is useful to consider three distinct types of potential surfaces, as shown in Figures 4a–c. In Figure 4a we have the case where two isomeric ions, A^+ and B^+, each exist in potential wells, but the barrier to interconversion of A^+ and B^+ is less than that required for unimolecular dissociation of either species. This situation can be uncovered by three experimental measurements. (i) The total energy of the system required to produce a given dissociation product will be the same irrespective of whether we start from A^+ or B^+, i.e., the rate-determining step is the attainment of a common transition state for dissociation, the energy requirement of which can be determined experimentally from appearance potential measurements. (ii) If the (fast) interconversion of A^+ and B^+ involves a hydrogen shift, then the rapid occurrence of this process can be investigated by deuterium labeling. (iii) Should ions initially generated as A^+ undergo two, or more, com-

(12) R. G. Cooks, personal communication.

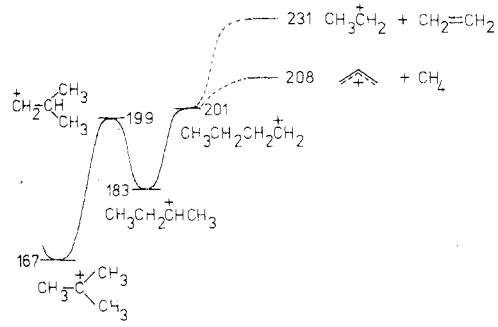

Figure 5. Potential surface for the unimolecular reactions of $C_4H_9^+$ cations. The ΔH_f values of the cations are taken from ref 16. Dissociation to the allyl ion and CH_4 from the normal configuration is arbitrarily chosen. Data in ref 15 indicate that the addition of CH_4 to the allyl ion involves an activation energy of 0–4 kcal mol^{-1} and that there are two channels for the reverse dissociation.

peting dissociations (which therefore must have similar activation energies), then ions initially generated as B^+ must also undergo the same competing dissociations in similar ratio(s).[13] This follows since ions initially generated as A^+ or B^+ must behave in the same way at the internal energies (hatched areas in Figure 4a) appropriate to dissociation(s).

A system which follows these criteria consists of the isomeric *n*-, *sec*-, iso-, and *tert*-butyl cations.[14] The ΔH_f values of these ions determine their relative positions on the energy scale of Figure 5. Irrespective of whether we generate *n*-, sec-, iso-, or *tert*-butyl cations at threshold, they undergo the reactions given in eq 3 and 4, in all cases allyl ion formation (96 ± 2%) dominating

$$n\text{-, } i\text{-, } sec\text{-, or } t\text{-}C_4H_9^+ \longrightarrow \begin{cases} CH_2{=}CH{-}CH_2^+ + CH_4 & (3) \\ C_2H_5^+ + C_2H_4 & (4) \end{cases}$$

over ethyl cation formation (4 ± 2%).

Interconversion of isomeric butyl cations prior to dissociation requires hydrogen and methyl shifts; the occurrence of such rapid shifts is supported by the statistical loss of CH_4, CH_3D, and CH_2D_2 in slow dissociations undergone by butyl-d_2 ions generated by loss of Br following ionization of $CH_3CH_2CD_2Br$.[14] Additionally, the measured transition-state energy for eq 3 is the same irrespective of whether we initially generate *n*-, iso-, or *sec*-butyl cations,[15] although there may be a subtlety of interpretation for CH_4 loss from t-$C_4H_9^+$.[15] However, there is no doubt that the various $C_4H_9^+$ cations do interconvert prior to slow unimolecular dissociations, and it is gratifying that, with only the reasonable assumption that 1,2-methyl and 1,2-hydrogen shifts do not involve activation energies where these processes are exothermic, the interconversions should indeed be rapid at the internal energies appropriate for dissociation to $C_2H_5^+$ or $C_3H_5^+$ (Figure 5).

It is clearly desirable to have a technique to indicate those ions which are formed in potential wells, as opposed to those which will collapse to more stable structures without activation energy. In this way, in the general case, the postulation of a small barrier to the interconversion of A^+ and B^+ in Figure 4a could be

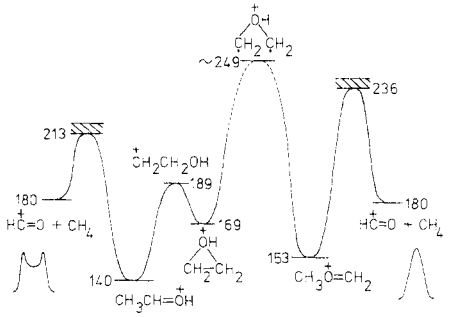

Figure 6. Potential-energy surface for the unimolecular reactions of $C_2H_5O^+$. The energy-release profiles for the loss of methane from two different reactant states are indicated at the appropriate parts of the surface.

checked. An excellent technique for making such a check has been developed, largely due to the work of Jennings[17] and McLafferty,[18] and has been extensively employed by McLafferty and co-workers. The method consists of selecting, after some 10^8 vibrations (i.e., in the "metastable region"), those ions which have not reacted within this time and dissociating them by collision with an inert gas. As we have seen, ions which remain undissociated after 10^8 vibrations will largely represent those with insufficient energy to undergo even the most facile unimolecular dissociation; some will be generated with such low internal energies that the $A^+ \rightleftharpoons B^+$ isomerization (Figure 4a) is not open to them. Therefore, some ions initially generated as A^+ must undergo collision as A^+; in theory, the energy imparted on collision opens the possibility of isomerization to B^+, but in practice the energy transferred to some A^+ is so large that fast direct dissociations of A^+ will preempt isomerization to B^+. Thus, the collision-induced spectrum of A^+ will be characteristically different from that of B^+.

In Figure 4b, we have the case where the barrier to interconversion of A^+ and B^+ is large compared to those for unimolecular dissociation of either. Clearly, the behavior of A^+ and B^+ will then be completely independent. Occasionally, the energy-release profile will indicate the isolated behavior of A^+ and B^+ even when the products of dissociation are the same. Thus, $CH_3CH{=}OH^+$ undergoes (as one of two unimolecular dissociations) CH_4 loss with a large kinetic-energy release, whereas the isomeric ion $CH_2{=}O^+CH_3$ loses CH_4 without a large kinetic-energy release[19] (see also Figure 6). Interconversion of $CH_3CH{=}OH^+$ and $CH_2{=}O^+CH_3$ would probably require the steps **10** ⇌ **14**. The highest energy species on such a surface would

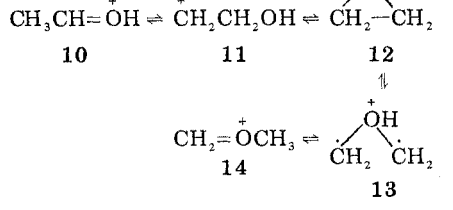

(13) H. M. Rosenstock, V. H. Dibeler, and F. N. Harlee, *J. Chem. Phys.*, **40**, 591 (1964).
(14) B. Davis, D. H. Williams, and A. N. H. Yeo, *J. Chem. Soc. B*, 81 (1970).
(15) J. L. Holmes, A. D. Osborne, and G. M. Weese, *Org. Mass Spectrom.*, **10**, 867 (1975).
(16) F. P. Lossing and G. P. Semeluk, *Can. J. Chem.*, **48**, 955 (1970).
(17) K. R. Jennings, *Int. J. Mass Spectrom. Ion Phys.*, 1, 227 (1968).
(18) (a) F. W. McLafferty, P. F. Bente, III, R. Kornfeld, S.-C. Tsai, and I. Howe, *J. Am. Chem. Soc.*, **95**, 2120 (1973); (b) F. W. McLafferty, R. Kornfeld, W. F. Haddon, K. Levsen, I. Sakai, P. F. Bente, III, S.-C. Tsai, and H. D. R. Schuddemage, *ibid.*, **95**, 3886 (1973); (c) F. W. McLafferty and I. Sakai, *Org. Mass Spectrom.*, **7**, 971 (1973).
(19) T. W. Shannon and F. W. McLafferty, *J. Am. Chem. Soc.*, **88**, 5021 (1966).

be **13**; on the basis of the known proton affinity of ethylene oxide and the assumption that the C–C bond strength in **12** is similar to that in cyclopropane, then ΔH_f(**13**) is estimated as ~249 kcal mol^{-1}, a level indeed much higher than that required for dissociation of either **10** or **14** (Figure 6).[20]

One anticipated consequence of the potential surface produced in Figure 6 is that the long-lived, ground-state $CH_3CH{=}OH^+$ ions which lie on this surface should be able to equilibrate with **11** and **12** prior to dissociation. Consequences of this equilibration are: (i) the carbon atoms pass through equivalent states, (ii) the hydrogens bound to carbon pass through equivalent states, and (iii) the hydroxyl hydrogen retains its identity. In agreement with these consequences, long-lived ions which dissociate to give the energy-release profile shown at the left hand side of Figure 6 (i) lose CH_4 and $^{13}CH_4$ from **15** in the ratio 1.06 ± 0.02, (ii) give CHO^+ and

$CH_3{}^{13}CH{=}\overset{+}{O}H$ (**15**) $\quad$ $CH_3CD{=}\overset{+}{O}H$ (**16**)

$CD_3CH{=}\overset{+}{O}H$ (**17**) $\quad$ $CH_3CH{=}\overset{+}{O}D$ (**18**)

CDO^+ from **16** in the ratio 2.83 (theory requires 3), (iii) give CDO^+ and CHO^+ from **17** in the ratio 3.17 (theory requires 3.0), and (iv) lose CH_3D from **18**.[21]

The chemistry of this ion becomes more complex when higher energy processes and fast reactions are considered.[21]

In Figure 4c, we have the situation where there is no direct dissociation of A^+, but A^+ isomerizes in a rate-determining step over a high barrier to B^+. The ion B^+ produced from A^+ has more internal energy than when B^+ is produced directly, and hence will behave in a different way. The main differences are likely to be: (i) The energy-release profile of B^+ produced from A^+ will be broader than that of B^+ produced directly. This is a consequence of some of the excess energy, $\epsilon^\ddagger$ (Figure 4c), fluctuating into the reaction coordinate at the instant of dissociation of B^+. (ii) B^+ produced from A^+ may undergo more reactions than B^+ produced directly, since the excess energy, $\epsilon^\ddagger$, may open up a new dissociation channel of B^+. Alternatively, if B^+ produced directly undergoes two competing dissociations (i.e., processes of similar activation energies), then B^+ produced from A^+ will undergo to a lesser extent the dissociation with the more ordered transition state. This follows since the presence of $\epsilon^\ddagger$ ensures that the dissociations following the slow isomerization will be fast; in the short time available, there will be discrimination against the dissociation requiring a more precise geometrical order.

These observable differences, if they occur, can then be supplemented by measuring the reaction energetics (appearance potential measurements), since dissociation products from A^+ (via B^+) must all have the same appearance potential; moreover, this measurement gives the height of the barrier to isomerization of $A^+ \rightarrow B^+$.

Two examples of the Figure 4c surfaces have so far been reported.[22,23] The dominant slow dissociations

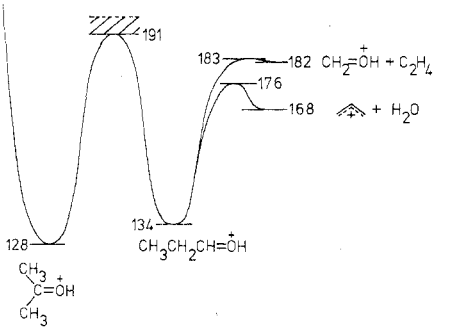

Figure 7. Partial potential surface for the dissociation of protonated acetone.

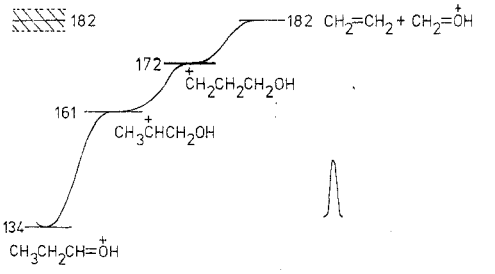

Figure 8. Proposed stepwise rearrangement and dissociation of $CH_3CH_2CH{=}OH^+$. The energy-release profile given in the figure corresponds to an average kinetic energy release of 0.74 kcal mol^{-1}.

of protonated acetone (**19**) are by loss of C_2H_4 and H_2O. The previously outlined criteria lead to the conclusion that **19** undergoes a rate-determining isomerization to protonated acetaldehyde (**19** → **20** → **21**) which then

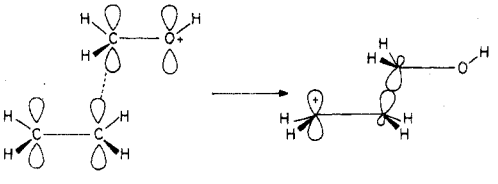

24 **25**

proceeds to $CH_2{=}OH^+ + C_2H_4$, probably as shown. The activation energy for the conversion **19** → **21** is ~63 kcal mol^{-1} (Figure 7).[23]

The most probable kinetic-energy release for the process **22** → **23** starting from **21** is only 0.74 kcal mol^{-1}, but this increases to 0.86 kcal mol^{-1} if the sequence is commenced from **19**. Only a small fraction (~1.5%) of the excess energy (~8 kcal mol^{-1}) appears in the reaction coordinate for the dissociation **22** → **23**; as might be expected, $\epsilon^\ddagger$ is very largely distributed in the other vibrational modes of the products.

Slow (metastable) unimolecular dissociations of directly generated **21** are via H_2O (88%) and C_2H_4 (12%) losses. Evidence for a more ordered transition state for the H_2O loss is found in the collisional activation spectrum of **21** where the H_2O/C_2H_4 loss is 41:59.[18c] Thus, there will be discrimination against the H_2O loss in the presence of excess energy, and indeed **21** formed from **19** undergoes H_2O and C_2H_4 losses in the abundances 31% and 69%.

The potential surface for the sequence **21** → **22** → **23** is reproduced in Figure 8 and leads to the expectation that the products of dissociation (produced directly

(20) G. Hvistendahl, R. D. Bowen, and D. H. Williams, unpublished work.
(21) B. G. Keyes and A. G. Harrison, *Org. Mass Spectrom.*, **9**, 221 (1974).
(22) G. Hvistendahl and D. H. Williams, *J. Am. Chem. Soc.*, **97**, 3097 (1975).
(23) G. Hvistendahl, R. D. Bowen, and D. H. Williams, *J. Chem. Soc., Chem. Commun.*, 294 (1976).

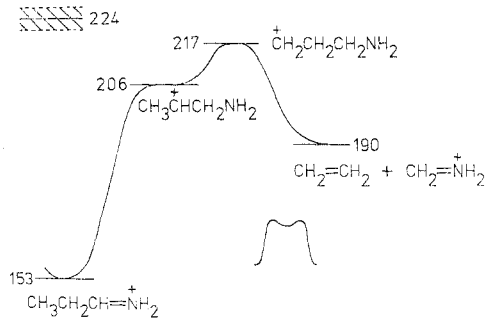

Figure 9. Proposed stepwise rearrangement and dissociation of $CH_3CH_2CH{=}NH_2^+$. The energy-release profile given in the figure corresponds to a kinetic-energy release of ~9 kcal mol^{-1}.

from **21**) might drift apart (as observed) rather than suffer mutual repulsion. Indeed, as $CH_2{=}OH^+$ approaches $CH_2{=}CH_2$ in the orientation shown in **24**, the

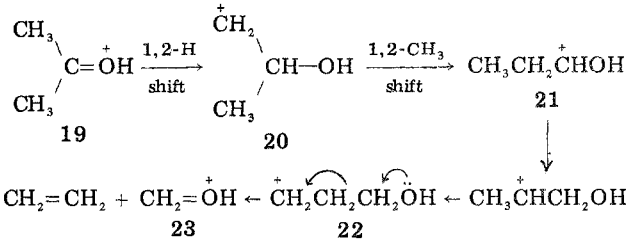

electronic energy of the system may continuously fall to produce the more stable adduct $^{+}CH_2CH_2CH_2OH$ (**25**). Experimental evidence that dissociation to C_2H_4 and $CH_2{=}OH^+$ does not involve a reverse activation energy is available from appearance potential measurements, which indicate an activation energy of 48 ± 3 kcal mol^{-1} for dissociation commencing from $CH_3CH_2CH{=}OH^+$ (see hatched area in Figure 8). Until we analyzed our unimolecular isomerizations and dissociations within the framework of the normal rules of mechanistic organic chemistry (calculating the heats of formation of presumed intermediates by a simple group equivalent method),[24] we had been intrigued by the observation that, if NH replaces O in the conversions **19** → **23** and **21** → **23**, C_2H_4 loss is still observed, but now occurs with a considerable release of kinetic energy (~9 kcal mol^{-1}).[25] However, the potential surface for the reactions of the protonated imine (Figure 9) shows that $^{+}CH_2CH_2CH_2NH_2$ should correspond to, or be near to, a transition state for the dissociative step.[26] From the linear $^{+}CH_2CH_2CH_2NH_2$ configuration, dissociation is strongly exothermic (~27 kcal mol^{-1}), and one-third of this exothermicity appears as mutual repulsion of the products. Experimental evidence that the reacting configuration, $^{+}CH_2CH_2CH_2NH_2$, has been correctly chosen is available from appearance potential measurements for $CH_2{=}NH_2^+$ production. These give a transition-state energy of 224 ± 4 kcal mol^{-1} (hatched area in Figure 9, i.e., an activation energy of 71 ± 4 kcal mol^{-1} starting from $CH_3CH_2CH{=}NH_2^+$), in reasonable agreement with the estimated ΔH_f value (217 kcal mol^{-1}) of $^{+}CH_2CH_2CH_2NH_2$. This last ion should of course be able to cyclize to protonated azetidine (ΔH_f = 154 kcal mol^{-1}), probably without activation energy, but the internal energies necessary for dissociation will allow reversion of the cyclization and suggest that the dissociation of protonated azetidine would be stepwise.

Conclusion

Unimolecular reactions occurring in the field-free regions of conventional magnetic sector mass spectrometers can be effectively studied to give detailed information on the chemistry of organic ions. Use of the microsecond time frame effectively filters out fast reactions, and probably most reactions which may involve excited states. Energy barriers to isomerization and dissociation steps can be determined under different circumstances, and kinetic-energy releases for dissociation are available. Isotope labeling (^2H and ^{13}C) is useful as a further experimental check on the proposed detail of a potential surface, and collisional activation experiments give information as to potential wells which exist on the surface.

The unimolecular experiments described above (which have largely been taken from our own work) have been kept to the minimum required to illustrate the principles involved. Much related work has not been cited because of the very nature of the Account, and limitations on space. Nevertheless, mention must be made of other contributions in this area, particularly those by Professors Cooks and Beynon,[1,2] McLafferty, Harrison, and Jennings (see references cited in this paper), and Holmes.[15,27,28]

Although information required for the construction of a unimolecular potential surface may on occasion be taken from bimolecular experiments (e.g., ion cyclotron resonance experiments to determine proton affinities), a discussion of such work has been specifically excluded from this Account.

I thank the Science Research Council for support of the work described and Drs. I. Howe and G. Hvistendahl and Mr. R. D. Bowen for recent important conceptional and practical contributions to the research. It is also a pleasure to acknowledge innumerable enlightening discussions, over the years, with the colleagues mentioned in the previous paragraph. Only through a blending of different areas of expertise has progress been possible.

(24) R. D. Bowen and D. H. Williams, *Org. Mass Spectrom.*, in press.
(25) N. Uccella, I. Howe, and D. H. Williams, *J. Chem. Soc. B*, 1933 (1971).
(26) D. H. Williams and R. D. Bowen, *J. Am. Chem. Soc.*, **99**, 3192 (1977).
(27) J. L. Holmes and G. Weese, *Org. Mass Spectrom.*, **9**, 618 (1974).
(28) J. L. Holmes and J. K. Terlouw, *Org. Mass Spectrom.*, **10**, 787 (1975).